ASIAN JOURNAL OF PHARMACEUTICAL SCIENCES 8 (2013) 11–18

Available online at www.sciencedirect.com

ScienceDirect

journal homepage: http://ees.elsevier.com/ajps/default.asp

Original Research Paper

A novel modified paclitaxel-loaded discoidal recombinant high-density lipoproteins: Preparation, characterizations and *in vivo* evaluation

Mengyuan Zhang, Junting Jia, Jianping Liu, Hongliang He, Lisha Liu*

Department of Pharmaceutics, China Pharmaceutical University, No. 24, Tong Jia Xiang, Nanjing 210009, China

ARTICLE INFO

Article history:
Received 25 December 2012
Received in revised form
14 January 2013
Accepted 1 February 2013

Keywords:
Modified d-rHDLs
Structural modification
LCAT
Remodeling
Drug leakage
Targeted drug delivery

ABSTRACT

This study is one of the first to focus on the unexpected drug leakage from discoidal recombinant high-density lipoproteins (d-rHDLs) as a consequence of remodeling process, mainly associated with lecithin-cholesterol acyltransferase (LCAT) during their metabolic process. Here, a newly monocholesterylsuccinate (CHS) modified paclitaxel-loaded d-rHDLs (cP-d-rHDLs) were constructed successfully through structural modification, thus aiming to improve the performance of d-rHDLs. And next their *in vitro* physiochemical properties and pharmacokinetics in Sprague–Dawley rats were elaborately investigated. Collectively our studies demonstrated that cP-d-rHDLs, whose remodeling behaviors were restrained effectively after structural modification, exhibited more excellent and promising properties as novel delivery vehicles for anti-cancer agents.

1. Introduction

High-density lipoproteins (HDLs) have recently attracted extensive attention as functional drug carriers owing to their attractive attributes [1], including favorable structure for incorporation of hydrophobic drugs, endogenesis, and the capacity to evade reticuloendothelial system (RES) thereby prolonging systemic circulation [2]. Additionally, the recognitions that the special receptor (scavenger receptor-BI, SR-BI),which is over-expressed in most malignant cells and mediate the selective uptake of HDLs, could provide strong support for the application of HDLs as a potential drug delivery system in cancer chemotherapy [3–5].

In the blood circulation, natural HDLs exist in two different structural forms known as discoidal HDLs (d-HDLs) and spherical HDLs (s-HDLs) (seen in Fig. 1) with unlike

* *Corresponding author*. Tel.: +86 2583271293, +86 13912955606 (mobile); fax: +86 2583271293.
E-mail address: jianpingliu1293@163.com (J. Liu).

Peer review under responsibility of Shenyang Pharmaceutical University

Production and hosting by Elsevier

1818-0876/$ – see front matter © 2013 Shenyang Pharmaceutical University. Production and hosting by Elsevier B.V. All rights reserved.
http://dx.doi.org/10.1016/j.ajps.2013.07.002

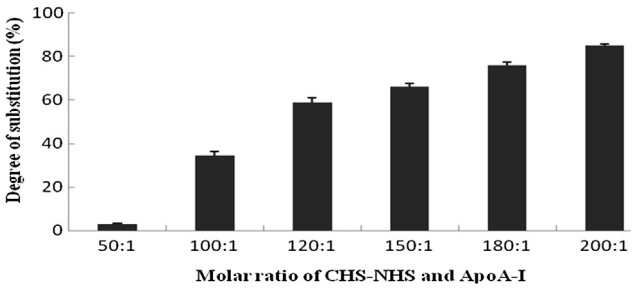

Fig. 1 – Degree of substitution of cA with different initial molar ratio of CHS-NHSE and ApoA-I from 50:1 to 200:1. (n = 3).

physical–chemical and biological properties of their own. Nascent d-HDLs obtain cholesterol from peripheral tissues and can be converted to mature s-HDLs induced by lecithin-cholesterol acyltransferase (LCAT) [6]. Because of the liposome-like structure, high affinity to SR-BI and an exclusive role in intracellular cholesterol efflux during reverse cholesterol transport (RCT) process thus hindering growth of tumor, recombinant d-HDLs (d-rHDLs) have been increasingly constituted as novel carriers for delivering anticancer agents [3,7–10]. However, previous studies by our team have found that drug-loaded d-rHDLs underwent the same remodeling behaviors *in vitro* as that of endogenous d-rHDLs under the action of LCAT [11], and the conversion evoked the leakage of encapsulated drugs before the carriers adhere to targeting cells, accordingly reduced the amounts of drugs exposed to cancer cells, further decreased drug efficacy and led to side effects [12]. Therefore, how to avoid the drug leakage ascribed to the remodeling behaviors of d-rHDLs has become an alarming problem to be solved urgently, especially for loading anticarcinogens.

On the ground of related literature, the essence of remodeling behaviors is that LCAT, the one of key plasma factors involved in the metabolism of d-rHDLs, catalyzes transacylation of the sn-2 fatty acid of phospholipid to the free hydroxyl group of cholesterol [13,14], thus generating cholesterol esters (CE), then CE migrates from bilayer lipid membrane to the center of d-HDLs constantly, resulting in the conversion of d-HDLs into mature s-HDLs [15]. Thus, removal of enzymatic substrates such as phospholipid or cholesterol to restrain the remodeling will be a promising outlet. However, for multivariant phospholipid of d-rHDLs, it is hardly possible to characterize the modified produce, consequently, modifying the only one hydroxyl group of cholesterol to avoid the destruction of d-rHDLs by LCAT is more reasonable.

In the current study, monocholesterylsuccinate (CHS) was synthesized and covalently conjugated to ApoA-I, successfully forming CHS modified ApoA-I (cA). Meanwhile, the degree of substitution, molecular weight and surface tension of cA were identified. Subsequently, the newly modified d-rHDLs composed of CHS, cA and phospholipid were prepared by thin-film dispersion and cholate dialysis methods. Two good reasons were responsible for this strategy: first, cholesterol was substituted by CHS to restrain the remodeling behaviors, second, ApoA-I, the important component recognized by SR-BI, was anchored to rHDLs through covalent binding with CHS, which was expected to increase binding efficiency of ApoA-I, and further achieve high tumor-targeting. Paclitaxel (PTX), a lipophilic antineoplastic agent was selected as the model drug. And *in vitro* characterizations of CHS-modified paclitaxel-loaded-discoidal rHDLs (cP-d-rHDLs) were systematically determined, which included particle size, zeta potential, drug entrapment efficiency, morphology and *in vitro* drug release of cP-d-rHDLs with and without LCAT. In addition, to further evaluate the effectiveness of structural modification, the pharmacokinetic behaviors of different PTX preparation, such as Taxol, PTX-loaded liposome (P-L), P-d-rHDL and cP-d-rHDLs were investigated in Sprague–Dawley rats, respectively. The ultimate purpose of our study was to improve the performance of d-rHDLs from a new perspective, and provide theoretical basis for enhancing the functionality of biomimetic drug delivery carriers in cancer chemotherapy.

2. Materials and methods

2.1. *Materials*

Paclitaxel was purchased from Yew Pharmaceutical Company Ltd. (Jiangsu, China). Taxol was prepared in our laboratory according to a commercial formulation. Lipoid S 100 was from Lipoid GmbH (Frigenstrasse 4, 67065 Ludwigshafen, Germany). Cholesterol was from Sigma–Aldrich (St. Louis, MO). All other chemicals of analytical or high-performance liquid chromatography (HPLC) grade were purchased from Chemical Reagent Company, Ltd. (Nanjing, China). Sephadex G50 was from Pharmacia (Sweden). ApoA-I was isolated from precipitate IV. Human plasma was supplied by Nanjing Red Cross (Nanjing, China). LCAT was isolated from human plasma in our laboratory.

2.2. *Synthesis and characterization of cA*

2.2.1. *Synthesis*

CHS was synthesized according to a previously reported protocol [16], which using cholesterol and succinic anhydride as raw materials in heptane and trace pyridine as a catalyst. After that, prepared CHS was covalently bound to the amino residues of ApoA-I to obtain the modified ApoA-I (cA) with some modifications [17] and the reaction procedure is shown in Scheme 1. Generally, the carboxyl groups of CHS were reactivated by twice equimolar amounts of 1-ethyl-3-(3-dimethylamino) propylcarbodiimide hydrochloride (EDC·HCl) and N-hydroxysuccinimide (NHS) in dichloromethane at 25 °C overnight, and the organic solvent was removed by evaporation. Then 0.5 mL of DMF containing various amounts of CHS–NHS active esters (CHE–NHSE) was added into ApoA-I solution by drop and allowed to agitate gently overnight at 4 °C. The reacted mixture was dialyzed against distilled water at room temperature for 2 days, followed by centrifugation at 12,000 rpm for 10 min to remove the extra active esters. Upon lyophilization, white product of CHS modified ApoA-I(cA) was obtained. A series of modified apolipoproteins designated as c_xA (where x was the input molar ratio of [CHS–NHS]/[ApoA-I]) were produced by changing the input molar ratio of CHS–NHSE to apolipoprotein from 50 to 200).

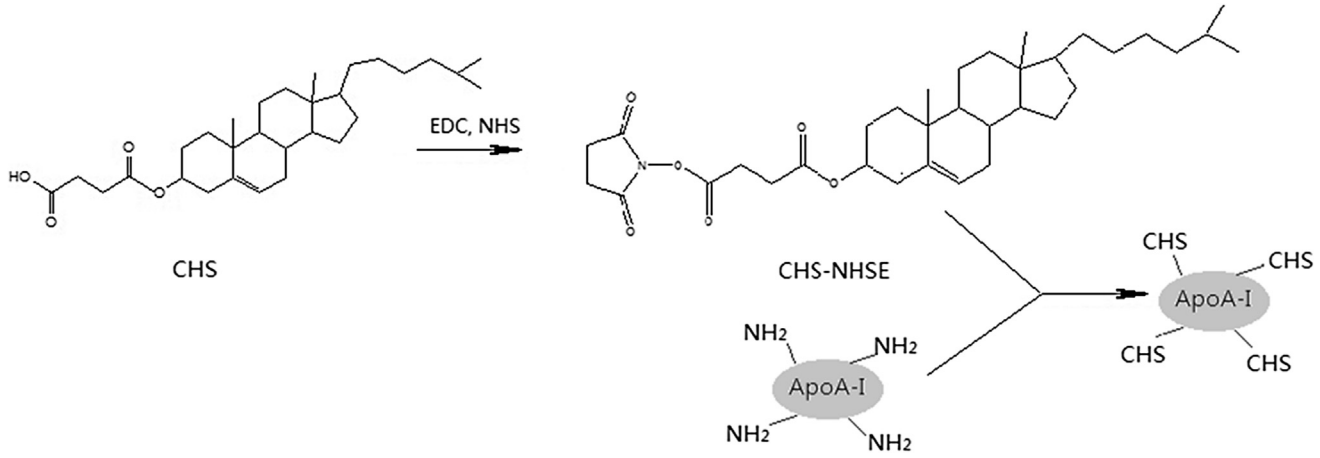

Scheme 1 – Synthetic scheme for monocholesterylsuccinate modified ApoA-I (cA).

2.2.2. *Evaluation of the degree of substitution of cA*

The trinitro benzene sulfonic acid (TNBS) method [18] was employed to define the degree of substitution of modified ApoA-I. In brief, ApoA-I and modified ApoA-I(cA) solution were diluted with PBS separately to obtain the samples with a series of concentrations (0.2–1.0 mg/mL). 0.2 mL $NaHCO_3$ (4% *w/v*, pH 8.5) and 0.2 mL TNBS (0.1%, *w/v*) were added to 0.2 mL of each sample, and mixed completely. The solution was then incubated in the dark for 2 h at 40 °C, and 0.2 mL SLS (10%, *w/v*) and 0.1 mL HCl (1 M)were subsequently added. After mixing completely, 0.2 mL of each sample was transferred to a 96-well plate, and the absorbance was recorded at 415 nm using a microplate reader (Multiskan MK3, Thermo Electron Corporation). The standard curves of ApoA-I and c_xA with different initial molar ratio (*x* ranges from 50 to 200)were obtained, and the degree of substitution was calculated according to the equation:

$$DS = \left(1 - \frac{K_{\text{modified apoA-I}}}{K_{\text{apoA-I}}}\right) \times 100\% \quad (1)$$

where DS is the degree of substitution; $K_{\text{apoA-I}}$ and $K_{\text{modified apoA-I}}$ are the slope rates of ApoA-I and cA, respectively.

2.2.3. *Determination of average molecular weight (MW) of cA*

Average molecular weight (MW) of cA was evaluated by sodium dodecyl sulfate-polyacrylamide gel electrophoresis (SDS-PAGE) gels. ApoA-I and $c_{120}A$ samples were diluted with treatment buffer, respectively. Then the mixtures were heated and loaded into the end of the gel wells, respectively. Electrophoresis of samples was performed on 12% resolving gel with 4% acrylamide stacking gel. After electrophoresis, the gel was stained with Coomassie blue R-250. Molecular weight of $c_{120}A$ was determined by comparing the relative mobility (distance traveled by the cA/distance traveled by the marker). The degree of substitution was expressed by the following equation:

$$DS_{cA} = \left(\frac{MW_{cA} - MW_{Apo-I}}{MW_{CHS} \times 120}\right) \times 100\% \quad (2)$$

where DS_{cA} is the degree of substitution; MW_{cA} is molecular weight of cA estimated by comparing with the marker. MW_{ApoA-I} and MW_{CHS} are 28,000 and 487, respectively.

2.2.4. *Measurement of surface tension of cA*

The surface tensions of ApoA-I and c_xA ($x = 50, 100, 120$) were measured by DCAT 2.1 tension meter (Dataphysics, Germany). Each sample was diluted appropriately with PBS prior to the measurements, and assayed in triplicate.

2.3. *Preparation of cP-d-rHDLs*

Generally, the preparation processes consisted of the construction of the lipid cores and subsequent formation of cP-d-rHDLs complexes by incubation of the lipid cores with cA induced by sodium cholate.

Thin-film dispersion method was taken to prepare the lipid cores of modified PTX-loaded d-rHDLs (cP-d-rHDLs) as described in our earlier study except that cholesterol was substituted by CHS [12]. Briefly, soy phosphatidylcholine (PC), CHS, and PTX with an optimized molar ratio of 50:1:2 based on drug entrapment efficiency were dissolved in dehydrated alcohol and dried in a rotary evaporator under vacuum to remove the solvent. The thin-film formed was hydrated in 0.01 M phosphate-buffered saline (PBS, pH 7.4) at room temperature by vortexing, followed by ultrasonication for 300 s using an Ultra-Homogenizer (JY 92II; Ningbo, China). The dispersions were subsequently extruded through 0.22 μm filters to obtain the fine suspensions containing modified PTX-loaded liposome (cP-liposome).

Thereafter, the cholate dialysis procedure [7] was employed to prepare cP-d-rHDLs. Briefly, $c_{120}A$ in PBS was added to the liposome suspensions under 600 rpm magnetic stirring at 4 °C, resulting in a final PC to $c_{120}A$ ratio around 1:10 (mol/mol). This selected degree of substitution of c_xA was based on the highest level of apolipoprotein-binding. Sodium cholate stock in PBS was added to mediate the later coupling of $c_{120}A$ to cP-liposome, resulting in a final PC to sodium cholate ratio around 1:1.6 (mol/mol). After incubation under constant magnetic agitation at 4 °C for 12 h, the mixtures were dialyzed against PBS for 48 h to remove free sodium cholate using dialysis bags (MW cutoff of 14,000 Da). At last, the resultant suspension was subjected to a pre-equilibrated Sepharose 4B column, and eluted with PBS (pH 7.4) to remove the unbound apolipoprotein.

The amounts of the modified apolipoprotein bound on the liposome were quantified by using Coomassie (Bradford) Protein Assay.

2.4. Characterization of cP-d-rHDLs

2.4.1. Particle size, zeta potential and drug entrapment efficiency

Particle size, zeta potential of cP-d-rHDLs and cP-liposomes were measured by dynamic light scattering (DLS) after the samples were diluted appropriately with aqueous phase.

Drug entrapment efficiency (EE) was determined using the microcolumn centrifugation method [12,19,20]. Briefly, cP-d-rHDLs suspension was added dropwise to the centre of a sephadex G50 microcolumn equilibrated with distilled water. Then centrifugation (500× *g*, 5 min) was applied to separate the loaded PTX in cP-d-rHDLs and free drug. cP-d-rHDLs particles were recovered through centrifugation while the free drug was retained in the Sephadex matrix. Ultimately, the concentrations of PTX incorporated into cP-d-rHDLs particles (C) and the initial total drug (C_0) were assayed by HPLC, respectively, after dilution with absolute ethanol. EE is calculated with the following formula:

$$EE(\%) = C/C_0 \times 100\% \quad (3)$$

2.4.2. Morphology observation of cP-d-rHDLs with and without LCAT

In order to investigate whether structural stability of cP-d-rHDLs was maintained 37 °C under the action of LCAT, morphological examination was performed by transmission electron microscopy (TEM, H-7650, Hitachi HighTechnologies Corporation). cP-d-rHDLs incubating with or without LCAT were diluted appropriately with aqueous phase before preparation for TEM. Each sample was dropped onto a copper grid coated with carbon film to form a thin film specimen, which was negatively stained with a drop of 2% (*w*/*v*) phosphotungstic acid and dried, then, visualized using TEM.

2.4.3. In vitro release of cP-d-rHDLs with and without LCAT

In order to investigate whether the drug leakage induced by LACT would be avoided, and further evaluate the effectiveness of structural modification, the release behaviors of PTX from the modified discoidal rHDLs with and without LCAT were characterized. Briefly, 0.5 mL of cP-d-rHDLs with or without LCAT were sealed in preswollen dialysis bags (molecular weight cutoff 12,000 Da). Then, dialysis bags were separately immersed in 200 mL of PBS (pH = 7.4) containing 0.1% (*w*/*v*) Tween 80 and incubated for 24 h at 37 °C on an orbital shaker. At specific time intervals, 0.5 mL of sample was withdrawn and replaced with the same amount of fresh release medium. After appropriate dilution with acetonitrile, the amount of PTX released from the preparations was determined by RP-HPLC.

2.5. In vivo evaluation: plasma pharmacokinetics in rats

2.5.1. Animals and drug administration

Twenty healthy adult male Sprague–Dawley rats (purchased from the Animal Breeding Center of Qinlong Mountain, Nanjing) weighing 200 ± 20 g (mean ± SD) were housed under standardized conditions with free access to food and water for 1 week. Prior to drug administration, all rats were kept for overnight fasting but allowed water ad libitum. All studies on animals were approved by the University Ethics Committee for Animal Experiments and conducted strictly in compliance with the National Guideline on the Care and Use of Laboratory Animals.

Rats were randomly divided into the following four groups ($n = 5$), respectively: (1) Taxol; (2) P-Ls; (3) P-d-rHDLs; (4) cP-d-rHDLs. The same dose of different preparations (7.5 mg/kg) was intravenously administrated through the tail vein of rats, respectively.

2.5.2. Collection and treatment of blood samples

The blood samples (0.4 mL) were collected from the plexus venous in eye ground at 5 min, 10 min, 15 min, 30 min, 1 h, 2 h, 4 h, 6 h, 8 h and 12 h post-dosing. 200 μL plasma sample was obtained by centrifugation at 3000 rpm for 10 min, and 10 μL of 1 mg/mL diazepam (internal standard) was added before vortex for 3 min. Each sample was mixed with 200 μL PBS (pH7.0) and acetidine, vortex-mixed for 3 min, centrifuged at 3000 rpm for 10 min. 0.9 mL of supernatant was collected, and dried under a nitrogen gas. The residue was then reconstituted in 100 μL methanol. After centrifugation for 10 min at 12,000 rpm, 20 μL of supernatant was recovered and injected into the HPLC system.

2.5.3. Chromatographic system

The plasma concentrations of PTX in rats were determined using a reversed-phase HPLC (Shimadzu LC-10A, Kyoto, Japan) system with a mobile phase composed of methanol:water (67:33, *v*/*v*) at a flow rate of 1.0 mL/min. A Kromasil ODS C_{18} column (5 μm, 150 mm × 4.6 mm) was utilized at 30 °C, and the detection wavelength was set at 227 nm.

2.6. Statistical analysis and in vivo–in vitro correlation (IVIVC)

All values are expressed as the mean ± standard deviation. Pharmacokinetic parameters were assessed with non-compartmental analysis using the DAS 2.0 software. The statistical significance of differences was analyzed by Student's *t*-test. Furthermore, IVIVC for P-d-rHDLs and cP-d-rHDLs was evaluated respectively.

3. Results and discussion

3.1. Degree of substitution, average molecular weight (MW) and surface tension of cA

As seen in Fig. 1, the degree of substitution significantly increased as the initial molar ratio of [CHS–NHSE]/[ApoA-I] increased ranging from 50 to 120; however, when the molar ratio was higher than 120, the degree of substitution increased at a diminished rate. Therefore, to maintain the biological activity of ApoA-I, c_{120}A with an acceptable degree of substitution (58.97%) was selected as a functional protein attached onto d-rHDLs.

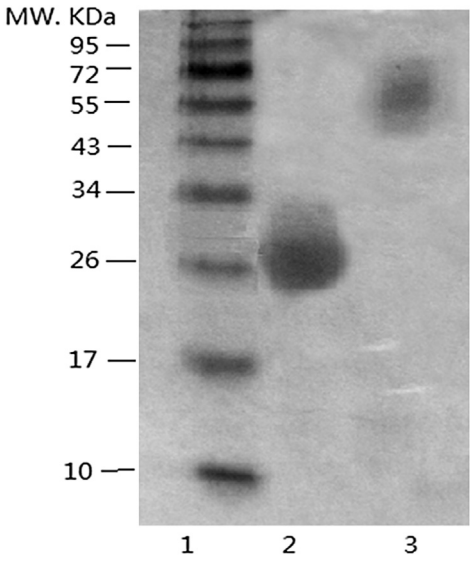

Fig. 2 – SDS-PAGE diagram of marker (lane 1), unmodified ApoA-I (lane 2).

As depicted in Fig. 2, SDS-PAGE revealed a markedly decreased migration distance for $c_{120}A$ compared with unmodified ApoA-I, indicating that CHS was conjugated to ApoA-I, resulting in an increase of molecular weight (MW). MW of $c_{120}A$ was estimated to be about 6300, and the degree of substitution was calculated to be 60%, which was in agreement with the data measured by TNBS methods.

Values of surface tension of modified ApoA-I (c_xA) shown in Fig. 3 were lower than that of unmodified ApoA-I. As the value of *x* increased, the corresponding surface tension decreased, which meant that the more amounts of CHS covalently binding to the protein, the stronger amphiphilicity and lower surface tension of protein were exhibited. Natural ApoA-I is soluble, the amphiphilicity of protein increased after modified with insoluble CHS, thus, the surface tension decreased [21]. The stronger amphiphilicity in addition to the cholesterol-derived structure in modified protein would facilitate cA to be anchored into liposomes.

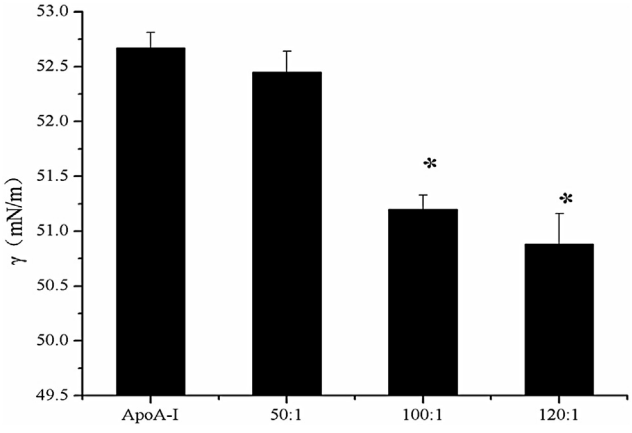

Fig. 3 – The surface tension of ApoA-I and c_xA ($x = 50, 100, 120$) with concentration of 0.2 mg/mL. (*$P < 0.01$ *vs.* ApoA-I) ($n = 3$).

3.2. *Characterization of CHS modified drug-loaded-discoidal rHDLs (cP-d-rHDLs)*

3.2.1. *Particle size, zeta potential and drug entrapment efficiency*

The particle size, zeta potential and drug entrapment efficiency of cP-d-rHDLs and cP-liposomes were given in Table 1, respectively. After incubation with cA, particle sizes of cP-liposomes were significantly decreased from 85.7 ± 3.71 nm to 22.3 ± 2.23 nm ($P < 0.01$), possibly because of the disappearance of internal hydrophilic cavities in liposomes under the action of cA and cholate [22]. And the smaller particle size of cP-d-rHDLs may enhance the residence time of drugs by preventing the glomerular filtration [23]. cP-d-rHDLs exhibited a 48% increment over cP-liposomes in negative surface charge, probably due to the presence of modified ApoA-I on the surface of liposomes. However, a non-significant reduction (−9%; $P < 0.05$) in EE was observed in cP-d-rHDLs, which was mainly associated with rapid formation of discoidal structures according to previous reports [12,24].

3.2.2. *Morphology observation of cP-d-rHDLs with and without LCAT*

To investigate whether structural stability of cP-d-rHDLs was maintained under the action of LCAT, TEM measurements were executed. Seen from the Fig. 4, a distinct multilayer discoidal structure of cP-d-rHDLs was displayed, even within LCAT solution, which was different from the conversion of P-d-rHDLs incubated with LCAT from discoidal to spherical structure reported by our earlier study [12]. This indicated that cP-d-rHDLs were successfully prepared, and the remodeling reaction induced by LCAT was restrained as we expected.

3.2.3. In vitro *release of cP-d-rHDLs with and without LCAT*

To investigate whether the drug leakage induced by LACT would be avoided, in vitro release study was performed. Fig. 5 illustrated *in vitro* PTX release profiles of P-d-rHDLs and cP-d-rHDLs with or without LCAT at different time points, respectively. cP-d-rHDLs suspension both with LCAT and without LCAT showed the slower release rate than that of P-d-rHDLs, which suggested that cP-d-rHDLs provided more effective sustained release of drugs than unmodified P-d-rHDLs. Furthermore, only 46.38 ± 1.48% and 46.61 ± 3.37% of PTX entrapped in cP-d-rHDLs with LCAT and without LCAT

Table 1 – Average diameter, zeta potential value and entrapment efficiency of cP-d-rHDL and cP-liposomes ($n = 3$).

	Formulation size (nm)	Zeta potential (mV)	EE (%)
cP-liposomes	85.7 ± 3.71	−18.46 ± 0.49	91.36 ± 2.08
cP-d-rHDL	22.3 ± 2.23**	−27.36 ± 2.31*	82.35 ± 4.16

Data are expressed as mean ± SD. *$P < 0.05$, **$P < 0.01$ *vs.* cP-liposomes.

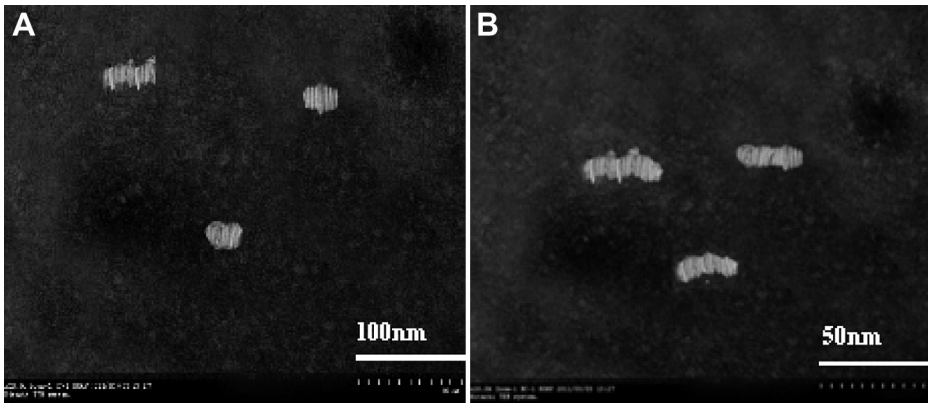

Fig. 4 – Microphotographs of different preparations using transmission electron microscope. (A) cP-d-rHDL without LCAT; (B) cP-d-rHDL incubation with LCAT.

were released in 24 h, respectively. Compared with the striking difference in the release behaviors between P-d-rHDLs with LCAT and without LCAT, the similar release behavior of drugs in cP-d-rHDLs with LCAT and without LCAT indicated that the drug leakage induced by LCAT was successfully prevented.

3.3. In vivo *evaluation: plasma pharmacokinetics in rats*

The plasma concentration–time profiles of four PTX different preparations in Sprague–Dawley rats after tail vein administration were shown in Fig. 6, and the obtained pharmacokinetic parameters were listed in Table 2. As shown in Fig. 6, there was a significant difference between the pharmacokinetic profiles of Taxol solution and other three suspensions, and no PTX was detectable only since 6 h after intravenous injection of Taxol. The pharmacokinetic behaviors of PTX were markedly altered after encapsulation in liposomal preparation, especially in cP-d-rHDLs. PTX in cP-d-rHDLs suspensions showed the slowest rate of elimination, followed by P-d-rHDLs, P-Ls and Taxol. It indicated that cP-d-rHDLs improved the stability of entrapped drugs in the blood circulation, and further prolonged the retention time. Moreover, a good IVIVC was also obtained for P-d-rHDLs and cP-d-rHDLs, respectively ($r = 0.892$ and 0.834).

As learned from Table 2, in comparison with Taxol, the other three preparations, showed prolonged mean residence time (MRT) ($P < 0.05$), which reflected the prolonged-release property of the three liposomes, especially cP-d-rHDLs. The values of area under the plasma concentration curve ($AUC_{(0-t)}$) for P-L, P-d-rHDLs and cP-d-rHDLs were 3, 4 and 5 times greater than that of PTX solution, respectively. Besides, for P-L, P-d-rHDLs and cP-d-rHDLs, distribution volume (Vd) was 1.41, 1.83, 2.30-fold lower than that of Taxol, and the corresponding total body clearance (CL) was 1.88, 4.73 and 8.01-fold lower than that of Taxol, respectively ($P < 0.001$), which indicated again that PTX incorporated in these particles, especially in cP-d-rHDLs, removed slowly from circulation compared to Taxol. Clearly, the conspicuous reduction of V and

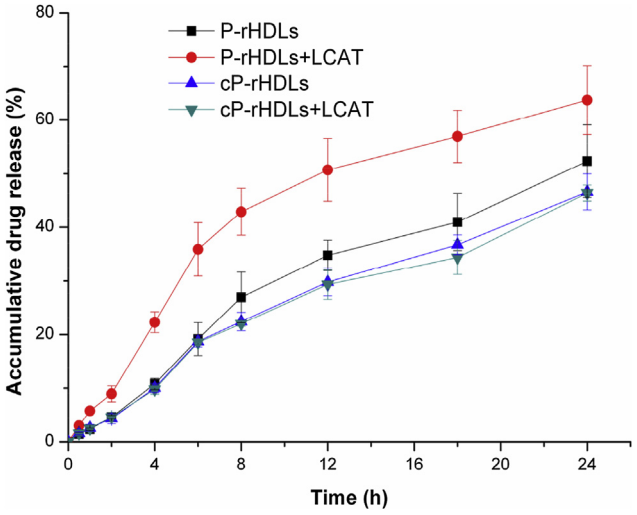

Fig. 5 – *In vitro* release profiles of PTX from different preparations using the dialysis-membrane methods. (■) P-d-rHDLs; (●) P-d-rHDLs + LCAT; (▲) cP-d-rHDLs; (▼) cP-d-rHDLs + LCAT. ($n = 3$).

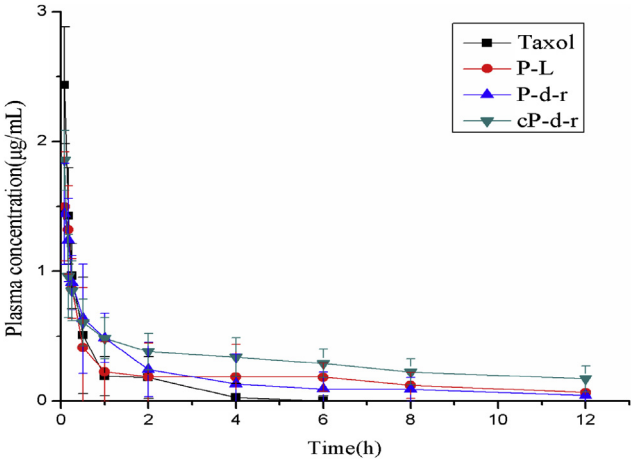

Fig. 6 – Mean plasma concentration vs. time curves of PTX in normal rats after i.v. administration of Taxol, P-liposomes, P-d-rHDLs and cP-d-rHDLs. (mean ± SD, $n = 5$).

Table 2 – Non-compartmental analysis of plasma data of PTX in normal rats after i.v. administration of Taxol, PTX-liposomes, P-d-rHDL and cP-d-rHDL (mean value ± SD, $n = 5$).

Preparations	$AUC_{0\to t}$ (μg/mL h)	MRT (h)	V (L)	CL (h/L)
Taxol	0.925 ± 0.076	0.916 ± 0.441	30.801 ± 6.933	10.825 ± 0.320
P-L	2.742 ± 1.562	4.081 ± 0.634*	21.822 ± 13.442	5.763 ± 1.490*
P-d-rHDLs	3.164 ± 0.062	7.280 ± 0.256*,△	16.859 ± 3.626*,△	2.290 ± 0.263*
cP-d-rHDLs	4.232 ± 1.075	10.266 ± 0.855*,△	13.394 ± 3.086*,△	1.351 ± 0.758*

*$P < 0.05$ Taxol vs. other formulations; △$P < 0.05$ P-L vs. other formulations.

CL suggested that cP-d-rHDLs effectively promote the uptake of PTX by specified tissue or cells, and it would be concluded that cP-d-rHDLs possessed a favorable targeting property.

4. Conclusion

The present work mainly concerns the exploitation of newly modified d-rHDLs to alleviate the drug leakage resulting from the remodeling behaviors of d-rHDLs in their metabolic process. The *in vitro* incubation test confirmed that the remodeling of d-rHDLs within LCAT was restrained by structural modification successfully. Moreover, pharmacokinetic studies in rats revealed that the potential of cP-d-rHDLs as novel targeting carriers. Further studies are planned to investigate whether cP-d-rHDLs can enhance the drug accumulation and diffusion in tumor cells, meanwhile their antitumor efficiency is specially worthy of note.

Acknowledgments

This study is financially supported by National Science Foundation Grant of China (No. 81072587), Jiangsu Province Ordinary College and University Innovative Research Programs (No. CXZZ11 0805), the Major Project of National Science and Technology of China for New Drugs Development (No. 2009ZX09310-004), and the Special Found Project of Universities' Basic Scientific Research of Central Authorities (No. ZJ11253). We also acknowledge the kind assistance of Tonrol Bio-Pharmaceutical Company, Ltd. for providing raw material to isolate apolipoproteins.

REFERENCES

[1] Rensen PCN, de Vrueh RLA, Kuiper J, et al. Recombinant lipoproteins: lipoprotein-like lipid particles for drug targeting. Adv Drug Deliv Rev 2001;47(2):251–276.
[2] Skajaa T, Cormode DP, Falk E, et al. High-density lipoprotein-based contrast agents for multimodal imaging of atherosclerosis. Arterioscl Throm Vas 2010;30(2):169–176.
[3] Mooberry LK, Nair M, Paranjape S, et al. Receptor mediated uptake of paclitaxel from a synthetic high density lipoprotein nanocarrier. J Drug Target 2010;18(1):53–58.
[4] Cho KH. Biomedicinal implications of high-density lipoprotein: its composition, structure, functions, and clinical applications. BMB Rep 2009;42(7):393–400.
[5] Lacko AG, Nair M, Prokai L, et al. Prospects and challenges of the development of lipoprotein-based formulations for anti-cancer drugs. Expert Opin Drug Deliv 2007;4(5):665–675.
[6] Rader DJ. Molecular regulation of HDL metabolism and function: implications for novel therapies. J Clin Invest 2006;116(12):3090.
[7] McConathy WJ, Nair MP, Paranjape S, et al. Evaluation of synthetic/reconstituted high-density lipoproteins as delivery vehicles for paclitaxel. Anti-Cancer Drugs 2008;19(2):183–188.
[8] Lacko AG, Nair M, Paranjape S, et al. High density lipoprotein complexes as delivery vehicles for anticancer drugs. Anticancer Res 2002;22(4):2045–2050.
[9] Corbin IR, Chen J, Cao W, et al. Enhanced cancer-targeted delivery using engineered high-density lipoprotein-based nanocarriers. J Biomed Nanotechnol 2007;3(4):367–376.
[10] McConathy WJ, Paranjape S, Mooberry L, et al. Validation of the reconstituted high-density lipoprotein (rHDL) drug delivery platform using dilauryl fluorescein (DLF). Drug Deliv Transl Res 2011;1(2):113–120.
[11] Wenli Z, Hongliang H, Jianping L, et al. Pharmacokinetics and atherosclerotic lesions targeting effects of tanshinone IIA discoidal and spherical biomimetic high density lipoproteins. Biomaterials 2012.
[12] Junting J, Yan X, Jianping L, et al. Preparation, characterizations, and *in vitro* metabolic processes of paclitaxel-loaded discoidal recombinant high-density lipoproteins. J Pharm Sci 2012;101(8):2900–2908.
[13] Calabresi L, Franceschini G. Lecithin: cholesterol acyltransferase, high-density lipoproteins, and atheroprotection in humans. Trends Cardiovasc Med 2010;20(2):50–53.
[14] Jonas A. Lecithin cholesterol acyltransferase. BBA-MOL Cell Biol L 2000;1529(1):245–256.
[15] Calabresi L, Favari E, Moleri E, et al. Functional LCAT is not required for macrophage cholesterol efflux to human serum. Atherosclerosis 2009;204(1):141–146.
[16] Shaikh VAE, Maldar NN, Lonikar SV, et al. Thermotropic liquid crystalline behavior of cholesterol-linked hydroxyethyl cellulose. J Appl Polym Sci 1999;72(6):763–770.
[17] Haque A, Kito M. Lipophilization of soybean glycinin: covalent attachment to long chain fatty acids. Agric Biol Chem 1982:46.
[18] Habeeb AFSA. Determination of free amino groups in proteins by trinitrobenzenesulfonic acid. Anal Biochem 1966;14(3):328–336.
[19] Wenli Z, Yan X, Jianping L, et al. Structure and remodeling behavior of drug-loaded high density lipoproteins and their atherosclerotic plaque targeting mechanism in foam cell model. Int J Pharm 2011;419(1):314–321.
[20] Jain SK, Chaurasiya A, Gupta Y, et al. Development and characterization of 5-FU bearing ferritin appended solid lipid nanoparticles for tumour targeting. J Microencapsul 2008;25(5):289–297.
[21] Xu Y, Jin X, Ping Q, et al. A novel lipoprotein-mimic nanocarrier composed of the modified protein and lipid for

tumor cell targeting delivery. J Control Release 2010;146(3):299–308.
[22] Oda MN, Hargreaves PL, Beckstead JA, et al. Reconstituted high density lipoprotein enriched with the polyene antibiotic amphotericin B. J Lipid Res 2006;47(2):260–267.
[23] Shi Y, Kim S, Huff TB, et al. Effective repair of traumatically injured spinal cord by nanoscale block copolymer micelles. Nat Nanotechnol 2009;5(1):80–87.
[24] Guo LS, Hamilton RL, Goerke J, et al. Interaction of unilamellar liposomes with serum lipoproteins and apolipoproteins. J Lipid Res 1980;21(8):993–1003.